VISCOSITY MODEL FOR SLAGS IN THE Al_2O_3-CaO-'FeO'- K_2O-Na_2O-MgO-SiO_2 SYSTEM

Evgueni Jak
The University of Queensland, Australia

ABSTRACT

A model has been developed that enables the viscosities of slags in the Al_2O_3-CaO-'FeO'-K_2O-Na_2O-MgO-SiO_2 system to be predicted within experimental uncertainties over a wide range of compositions and temperatures. The Eyring equation is used to express viscosity as a function of temperature and composition. The model links the vaporisation and activation energies in the slag viscosity expression to the slag internal structure through the concentrations of various $Si_{0.5}O$, $Me^{n+}_{2/n}O$ and $Me^{n+}_{1/n}Si_{0.25}O$ viscous flow structural units. The concentrations of these structural units are derived from a quasi-chemical thermodynamic model of the liquid slag using FactSage computer package and ChemApp software. The model describes a number of slag viscosity features including the charge-compensation effect specific for the Al_2O_3-containing systems. The predictive capability of the model is discussed with reference to the physical basis of the model parameters.

An example of an application of the new viscosity model to predict viscosity changes in slags inside the iron blast furnace due to re-circulation of volatile elements (Na and K) is given.

INTRODUCTION

Slag viscosity is a key property essential for a number of metallurgical and power generation industrial processes. Development of a reliable and general model that would enable the viscosities of multi-component slag systems to be predicted over wide ranges of compositions and temperatures has been undertaken at the Pyrometallurgy Research Centre over a number of years [1, 2, 3, 4, 5, 6, 7]. In the present paper a general, structurally-based viscosity model for fully liquid silicate slags in the Al_2O_3-CaO-'FeO'-K_2O-Na_2O-MgO-SiO_2 system is outlined and recent developments of the model are described. There are other examples of structurally-based viscosity model developments [8, 9, 10, 11].

MODEL

$$h = \frac{2RT}{\Delta E_v} \frac{(2\pi m_{SU} kT)^{1/2}}{v_{SU}^{2/3}} \exp\left(\frac{E_a}{RT}\right) \quad (1)$$

$$m_{SU} = m_{Si\text{-}Si} X_{Si\text{-}Si} + m_{Me\text{-}Si} X_{Me\text{-}Si} + m_{Me\text{-}Me} X_{Me\text{-}Me} \quad (2)$$

$$V_{SU} = v_{Si\text{-}Si} X_{Si\text{-}Si} + v_{Me\text{-}Si} X_{Me\text{-}Si} + v_{Me\text{-}Me} X_{Me\text{-}Me} \quad (3)$$

$$E_a = E_{a,Si\text{-}Si} X_{Si\text{-}Si} + E_{a,Me\text{-}Si} X_{Me\text{-}Si} + E_{a,Me\text{-}Me} X_{Me\text{-}Me} \quad (4)$$

$$\Delta E_v = \Delta E_{v0} \exp\left(\varepsilon_{v.Si\text{-}Si} X_{Si\text{-}Si} + \varepsilon_{v.Me\text{-}Si} + X_{Me\text{-}Si} + \varepsilon_{v.Me\text{-}Me} X_{Me\text{-}Me}\right. \quad (5)$$

Frenkel's kinetic theory of liquids [12, 55, 56] considers a liquid to possess a solid-like structure with molecules, or more generally, structural units (SU), oscillating near average positions in their energetic cells (potential wells), with oscillations, which are higher in magnitude than the potential barrier, resulting in the movement of a structural unit (SU) into an adjacent cell, provided the latter is vacant. These vacant cells, or *holes*, formed in the liquid as a result of fluctuations, are distributed randomly throughout the liquid. The viscosity of liquid as a reaction to the applied shear force then is determined by two factors: the ability of structural unit to jump over the potential barrier and the presence of *holes* in the liquid. The Eyring viscosity equation was derived [13, 57, 58] using these principles [12, 55, 56] (see Equation 1), where R [J/K/mol] and k [J/K] are the gas and the Boltzmann constants, $\pi \approx 3.1416$, T is the absolute temperature [K], ΔE_v and E_a [J/mol] are the vaporisation and activation energies, m_{SU} [kg] and v_{SU} [m^3] are the average mass and volume of a viscous flow structural unit. The activation energy E_a reflects the interactions between different structural units composing the liquid. The energy of vaporisation ΔE_v is related to the free volume of the liquid, i.e., to the concentration of the holes in the liquid determined by the energy of the hole formation, and can be approximately related to the latent heat of vaporisation.

Equation 1 requires definition of a viscous flow structural unit and contains four parameters dependent on this definition: mass and volume of a structural unit, activation energy, and energy of vaporisation. These parameters are clearly related to the internal structures of liquids, types of structural units and interactions between them.

Conventional description of complex silicate slag structure includes the silicate network of SiO_4^{4-} tetrahedra broken by different metal cations that are distributed to keep the total electroneutrality [14-15]. A silicate slag may also be considered as a nearly close-packed arrangement of larger oxygen anions with smaller metal cations that occupy the

interstices and interact with each other [14]. Fincham and Richardson [16] suggested that properties of a silicate slag can be related to the concentrations of three different types of oxygens: *bridging* (O^0 – connected to two silicon cations), *non-bridging* (O^- – connected to only one silicon), and *free* (O^{2-} – associated with non-silicon cations). Figure 1 gives a simplified two-dimensional schematic picture of the internal structure of the slag that follows from these concepts. Derived from the above background, in the present model the viscous flow of the silicate slag is considered to be a movement of oxygens together with metal cations partly associated with them under the applied shear force (see Figure 1) so that the viscous flow structural units are defined as oxygen anions with metal cations partly associated with them (see ovals in Figure 1). e.g. $Si_{0.5}O$ (= Si-O-Si = Si-Si), $Me^{n+}{}_{2/n}O$ (= Me-O-Me = Me-Me) and $Me^{n+}{}_{1/n}Si_{0.25}O$ (= Me-O-Si = Me-Si), where n is the oxidation state of a metal cation Me^{n+}. These viscous flow structural units differ from the conventional structural units [14, 15, 16], however, for simplicity, they will be referred to as just *structural units*.

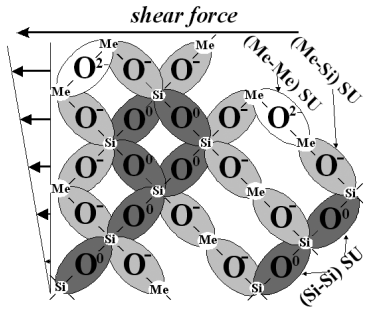

Figure 1: Internal structure and viscous flow structural units (SU) in silicate melts (0^0, 0^-, and 0^{2-} - non-bridging, bridging, and free oxygens)

There are a number of different types of structural units that involve oxygen associated with various combinations of metal cations. For example, for the binary MeO-SiO_2 silicate slag (see Figure 1) three types of structural units can be identified (Si-O-Si) (shaded with dark grey), (Me-O-Si) (shaded with light grey) and (Me-O-Me) (white, not shaded). Their concentrations are indicated as $X_{Si\text{-}Si}$, $X_{Me\text{-}Si}$ and $X_{Me\text{-}Me}$, respectively. The ΔE_v, E_a, m_{SU} and v_{SU} values in the present model are expressed through the respective molar fractions of the various structural units $X_{Si\text{-}Si}$, $X_{Me\text{-}Si}$, and $X_{Me\text{-}Me}$ present in the melt. The average mass and volume of structural units are expressed with Equations 2 and 3, where $m_{Si\text{-}Si}$, $m_{Me\text{-}Si}$, $m_{Me\text{-}Me}$ and $v_{Si\text{-}Si}$, $v_{Me\text{-}Si}$, $v_{Me\text{-}Me}$ are the masses and volumes of the respective structural units. The $v_{Si\text{-}Si}$, $v_{Me\text{-}Si}$ and $v_{Me\text{-}Me}$ values are calculated using the effective diameters of structural units estimated from the ionic radii of various ions (O, Si, Me) composing a particular structural unit; the ionic radii are taken from Shannon [17]; the angles between different bonds within a structural unit are not taken into account. In the binary system MeO-SiO_2 the integral molar activation energy E_a is expressed through the corresponding partial molar activation energies $E_{a,Si\text{-}Si}$, $E_{a,Me\text{-}Si}$ and $E_{a,Me\text{-}Me}$ (see Equation 4). The vaporisation energy ΔE_v is described by an exponential function (see Equation 5), where $E_{v0=1}$ J/mol and $\varepsilon_{v,Si\text{-}Si}$, $\varepsilon_{v,Me\text{-}Si}$ and $\varepsilon_{v,Me\text{-}Me}$ are the dimensionless *partial* vaporisation energy coefficients of each type of structural unit.

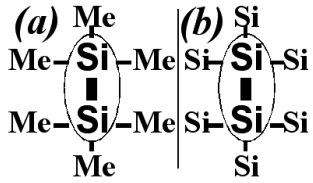

Figure 2: Different neighbours of (Si-O-Si) structural units (oxygen anions are not shown)

In addition to one oxygen a given structural unit also involves and two metal cations, which have other neighbours and are involved into other structural unit(s). The forces holding the first considered structural unit and therefore corresponding partial molar activation energy then depend on the type of neighbours. For example, if the two Si cations forming a (Si-O-Si) structural unit have other Me cations as neighbours (Figure 2a), they will have a different partial activation molar energy compared to a case when some or all other neighbours are also silicons (e.g. Figure 2b). The effect of neighbouring structural units on a given partial activation energy is expressed as a function of the concentrations of other types of structural units, so the partial molar activation energy of each type of a structural unit in the Equation (4) was expressed using Equations (6-8). Only the effect of the second nearest neighbours is usually taken into account in the model. For example, $E_{a,Si\text{-}Si}$ does not depend on $X_{Me\text{-}Me}$ and vice versa, because (Me-O-Me) structural unit cannot be the closest neighbour of the (Si-O-Si) structural unit. The description of experimental data required an introduction of a higher power term $X^2_{Si\text{-}Si}$, and that the binary contributions of nearest neighbours to most of the partial activation energies except $E_{a,Si\text{-}Si}$ can be neglected. The partial activation energies $E_{a,Me1\text{-}Me2}$ for the slag systems with limited or no experimental data available (e.g. Al_2O_3-'FeO' and CaO-'FeO') were taken to be equal ½ ($E_{a,\ Me1\text{-}Me1} + E_{a,\ Me2\text{-}Me2}$). The dimensionless partial vaporisation energies $\varepsilon_{v,Si\text{-}Si}$, $\varepsilon_{v,Me\text{-}Si}$ and $\varepsilon_{v,Me\text{-}Me}$ are described in a similar way.

$$E_{a,Si-Si} = E^{0}_{a,Si-Si} + E^{Si-Si,1}_{a,Si-Si} X_{Si-Si} + E^{Si-Si,2}_{a,Si-Si} X^{2}_{Si-Si} + E^{Me-Si}_{a,Si-Si} X_{Me-Si} \quad (6)$$

$$E_{a,Me-Si} = E^{0}_{a,Me-Si} + E^{Me-Si}_{a,Me-Si} X_{Me-Si} + E^{Si-Si}_{a,Me-Si} X_{Si-Si} + E^{Me-Me}_{a,Me-Si} X_{Me-Me} \quad (7)$$

$$E_{a,Me-Me} = E^{0}_{a,Me-Me} + E^{Me-Me}_{a,Me-Me} X_{Me-Me} + E^{Me-Si}_{a,Me-Me} X_{Me-Si} \quad (8)$$

In the present work the concentrations of structural units are determined using the quasi-chemical thermodynamic model of the slag developed by Blander and Pelton [18, 19, 20] and incorporated in the computer system FactSage [21]. The modified quasi-chemical model [18, 19, 20] takes into account short-range ordering of second-nearest-neighbour-cations in the ionic melt. For a binary MeO-SiO_2 slag the quasi-chemical model considers the formation of two nearest-neighbour pairs (Me-Si) from a (Me-Me) and a (Si-Si) pair, which are also called second nearest neighbour bonds (SNNB) [18, 19, 20]. Figure 1 illustrates for the binary MeO-SiO_2 system that the concentrations of the various types of the viscous flow structural units participating in the viscous flow are equal to the concentrations of the corresponding second nearest neighbour bonds of the quasi-chemical thermodynamic model [18, 19, 20]. Since its development the quasi-chemical model as part of the FactSage computer package [21] has been successfully applied to describe experimental phase equilibria, thermodynamic and other types of data in

many slag systems, from binary to multi-component systems. The SNNB distributions calculated with the quasi-chemical thermodynamic model may be taken as a reasonable approximation of the internal structures of the slags. The important point here is that, in constructing the quasi-chemical thermodynamic model of the liquid slag, valuable information about the structure of this phase at the atomic level can be obtained. This information can then be used as a basis for the description of physicochemical properties. The new thermodynamic database of the system Al-Ca-Fe-K-Mg-Na-O-Si [22, 23] has been used. The new thermodynamic database [22, 23] incorporates the latest experimental data, uses advanced thermodynamic models of the solid and liquid oxide phases, and is the result of the systematic thermodynamic optimisation of the binary, ternary, and multi-component systems. SNNB concentrations were calculated using FacSage [21] with the new database [22, 23] and ChemApp [24].

The predicted SNNB concentrations and trends were carefully analysed. Examples of SNNB distributions for binary silicate systems are given in Figure 3, showing that the so-called ordering (preference to form Me-Si over Me-Me and Si-Si SNNB) decreases from the Na_2O-, K_2O- and CaO- to MgO-, *FeO*- and Al_2O_3–silicate system. It is important that the model parameters were selected using restrictions and trends in the activation and vaporisation energies discussed in the following section. Systematic optimisation of the systems was carried out in cycles from lower order systems to the multi-component data until satisfactory agreement with all accepted experimental data was achieved. Table 1 reports present model parameters, which contains some parameters previously reported [1, 2, 3, 4, 5, 6, 7] and modified parameters.

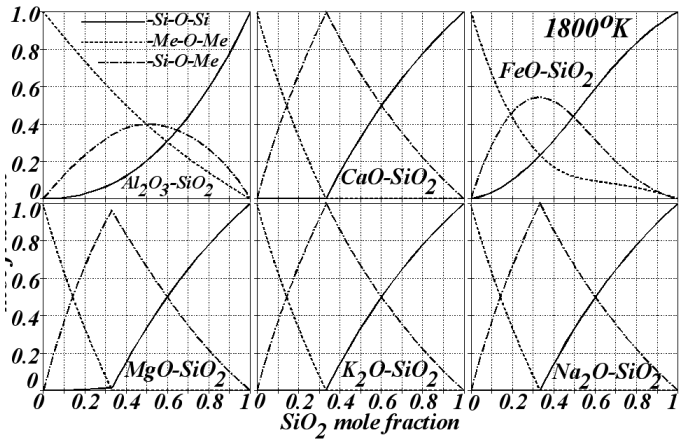

Figure 3: Concentrations of bond fractions at 1800°K predicted by FactSage

Table 1: The viscosity model parameters

The average mass and volume of structural units

SU	Si-Si	Al-Al	Ca-Ca	Fe-Fe	K-K	Mg-Mg	Na-Na	KAlO-KAlO	NaAl-NaAl	Si-Al	Si-Ca	Fe-Si	Si-K2	Mg-Si	Na-Si
m,SUx10^{-26}kg	4.99	5.64	9.31	11.93	15.64	6.69	10.29	16.29	13.61	5.32	7.15	8.46	10.32	5.84	7.64

MP,SU	Si-KAlO	Si-NaAl	Ca-Al	Fe-Al	Al-K2	Al-KAlO	Mg-Al	Na-Al	Al-NaAl	Fe-Ca	Ca-K	Ca-KAlO	Mg-Ca	Na-Ca	Ca-NaAl
m,SUx10^{-26} kg	10.64	9.30	7.48	8.79	8.79	10.97	6.17	7.97	9.63	10.62	12.48	12.80	8.00	9.80	11.46
v,SUx10^{-29}m^3	6.29	5.15	4.27	3.65	5.49	7.49	3.49	4.32	6.12	5.03	7.28	9.67	4.84	5.86	8.04

MP,SU	Fe-K	Mg-Fe	Fe-Na	Mg-K	Na-K	Mg-Na	Fe-KAlO	K-KAlO	Na-NaAl	Fe-NaAl	K-NaAl	Mg-KAlO	Mg-NaAl	Na-KAlO	KAl-NaAl
m,SUx10^{-26}kg	13.79	9.31	11.11	11.17	12.97	8.49	14.11	15.96	11.95	12.77	14.63	11.49	10.15	11.95	14.95
v,SUx10^{-29}m^3	6.39	4.16	2.40	6.16	7.47	4.90	8.59	11.74	8.13	7.09	9.88	8.41	6.84	9.88	12.91
v,SUx10^{-29}m^3	1.92	3.03	5.79	4.34	9.00	3.99	5.94	14.98	10.81	2.43	3.50	2.96	4.58	2.83	3.56

The viscosity activation and vaporisation average energy coefficients [J mol^{-1}]

$E_{a,Si\text{-}Si} = 80900 + 464963X^2_{Si\text{-}Si} + 498451X_{Si\text{-}Al} + 233696X_{Si\text{-}Ca} + 516645X_{Fe\text{-}Si} + 277000X_{Mg\text{-}Si} + 210000X_{Si\text{-}K}$

$-320000X^{1/5}_{Si\text{-}K}X^5_{Si\text{-}Si}+500000X^2_{Na\text{-}Si}-270000X^{1/5}_{Na\text{-}Si}X^5_{Si\text{-}Si}+436800X_{Si\text{-}KAl}+600000X_{Si\text{-}NaAl}$;

$E_{a,Al\text{-}Al}$ =129911; $E_{a,Ca\text{-}Ca}$ = 82126; $E_{a,Fe\text{-}Fe}$ = 49504; $E_{a,K\text{-}K}$ = 35000; $E_{a,Mg\text{-}Mg}$ =105890;

$E_{a,Na\text{-}Na}$ = 30000;

$E_{a,Si\text{-}Al} = 277533+73759X_{Si\text{-}Ca}-270000X_{Fe\text{-}Si}+562671X_{Al\text{-}Ca}+743000\ X_{Al\text{-}Fe}$;

$E_{a,Si\text{-}Ca} = 119885-7300X_{Fe\text{-}Si}-20000X_{K\text{-}Si}+18540X_{Mg\text{-}Si}-90000X_{Na\text{-}Si}+29000X_{Al\text{-}Ca}+37000X_{Fe\text{-}Ca}$;

$E_{a,Si\text{-}Fe} =28120+95145X_{Mg\text{-}Si}+120000X_{Fe\text{-}Al}-753000X_{Fe\text{-}Ca}-180000X_{Mg\text{-}Fe}$; $E_{a,Si\text{-}K}$=50000;

$E_{a,Si\text{-}Na}$ = 50000;

$E_{a,Si\text{-}Mg} =100420+150000X_{Mg\text{-}Al}+100000X_{Mg\text{-}Ca}+270000X_{Mg\text{-}Fe}$; $E_{a,Al\text{-}Fe}$ = 99708;

$E_{a,Al\text{-}Mg}$=132651;

$E_{a,Si\text{-}KAl} = 403200-70000X_{Si\text{-}Al}+10000X_{Si\text{-}Ca}-200000X_{Fe\text{-}Si}$; $E_{a,Ca\text{-}Al} = 183400-1780X_{Fe\text{-}Al}+55771X_{Al\text{-}Mg}$;

the rest $E_{a,Me1\text{-}Me2}$, = $0.5(E_{a,Me1\text{-}Me1} + E_{a,Me2\text{-}Me2})$

$\varepsilon_{a,Si\text{-}Si} = 17.34+11.12X_{Si\text{-}Si}-6.22X^2_{Si\text{-}Si}+1.06X_{Si\text{-}Al}+0.06X_{Fe\text{-}Si}+0.05X_{Mg\text{-}Si}+1.80X_{Si\text{-}K}+1.80X_{Si\text{-}Na}$;

$\varepsilon_{a,Al\text{-}Al}$ =13.59; $\varepsilon_{a,Ca\text{-}Ca}$ =13.02; $\varepsilon_{a,Fe\text{-}Fe}$ =11.25; $\varepsilon_{a,K\text{-}K}$ =11.00; $\varepsilon_{a,Mg\text{-}Mg}$ =13.85; $\varepsilon_{a,Na\text{-}Na}$ =11.00;

$\varepsilon_{a,Si\text{-}Al}$ =20.08+9.00XCa-Si; $\varepsilon_{a,Si\text{-}Ca}$ =14.46; $\varepsilon_{a,Si\text{-}Fe}$ =9.60+6.00$X_{Mg\text{-}Si}$; εa,Si-K =11.00;

$\varepsilon_{a,Si\text{-}Mg}$ =13.33;

$\varepsilon_{a,Si\text{-}Na}$ =12.30; $\varepsilon_{a,Si\text{-}KAl}$ =22.50; $\varepsilon_{a,Si\text{-}NaAl}$ =22.70; $\varepsilon_{a,Al}$-=16.88;

the rest $\varepsilon_{a,Me1\text{-}Me2}$, = $0.5(\varepsilon_{a,Me1\text{-}Me1} + \varepsilon_{a,Me2\text{-}Me2})$

The recent changes to the viscosity model and some of the modifications have recently been introduced are briefly outlined below.

MODELLING OF VISCOSITIES IN THE Na_2O- AND K_2O- CONTAINING SILICATE SYSTEMS

The measured viscosities decrease sharply as Na_2O and/or K_2O are added to the high-silica slags (see Figures 4 and 5). For example, addition of 5 mol % of Na_2O to the silica at 1600ºC results in the drop of the viscosity from 13188270 to 151 Pa*s - by over 87,000 times (see Figure 4).

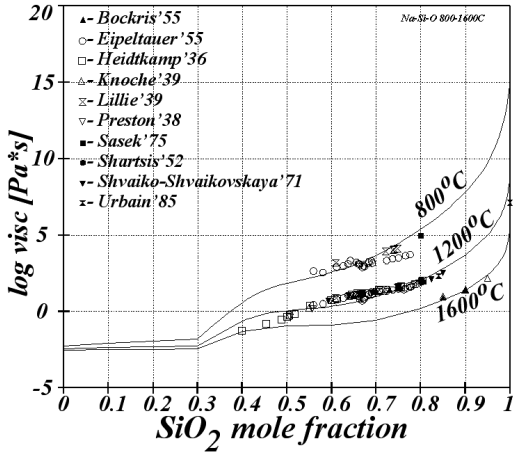

Figure 4: Viscosities in the Na-O-Si system

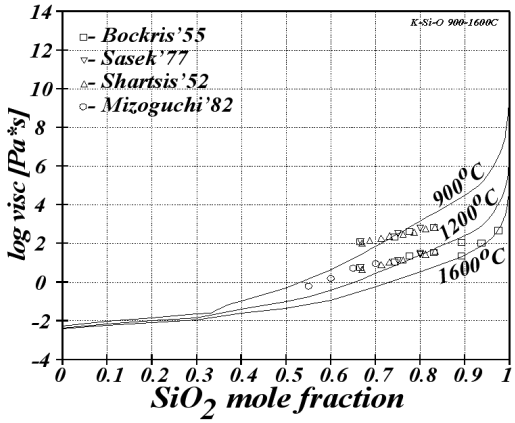

Figure 5: Viscosities in the K-O-Si system

Similarly, addition of 2.5 mol % of K_2O to the silica at 1600ºC results in the drop of the viscosity by over 10,000 times (see Figure 5). This decrease in viscosity is much greater compared to other metal oxides previously modelled (see Figure 6 for comparison of predicted viscosities in binary silicate systems) and could not be described with previously-introduced maximum second power term $X^2_{Si\text{-}Si}$ [1, 2, 3, 4, 5, 6, 7]. Additional $X^{1/z}_{Na\text{-}Si}$ $X^z_{Si\text{-}Si}$ and $X^{1/z}_{K\text{-}Si}X^z_{Si\text{-}Si}$ terms (z = 5) were introduced to describe experimental data. The agreement of the model with current set of model parameters (Table 1) with experimental data in the Na_2O-SiO_2 [see ref. 25 to 34] and K_2O-SiO_2 [32, 33, 34, 35, 36] systems is illustrated in Figures 4 and 5.

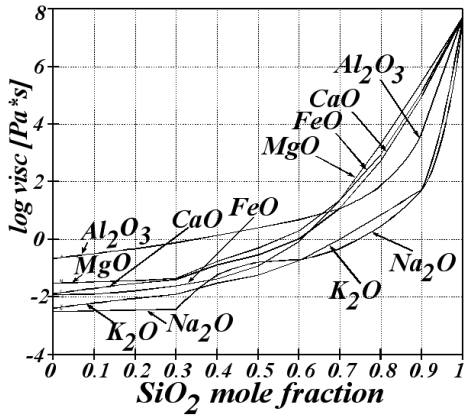

Figure 6: Viscosities in the Me-O-Si systems predicted by the present model

Charge Compensation Effect

Experiments indicate that the viscosities in the Al-containing Al_2O_3-(Me^+, Me^{2+})$_x$O-SiO_2 silicate slag systems go through the maximum values with increasing (Me^+,Me^{2+})O/Al_2O_3 ratio at $X_{MeO}/X_{Al2O3} \approx 1$, for example, in the Al-Ca-O-Si [39, 40], Al-Mg-O-Si [38], Al-Na-O-Si [34, 44, 45, 46] and Al-K-O-Si [41, 42] systems. This maximum is attributed [47] to the so called *charge compensation effect* comprising of the Al^{3+} cation's ability to take the tetrahedral interstitial between the oxygen anions if the excess negative charge for Al^{3+} is compensated by the alkali or alkaline earth cations, consequently forming Me^+AlO_2 or $Me^{2+}Al_2O_4$ associates in the melt. The previous thermodynamic quasi-chemical model did not describe the charge compensation effect [48]. In order to describe the viscosity behaviour (maximum at $X_{MeO}/X_{Al2O3} \approx 1$) in the CaO, FeO and MgO-containing systems a special charge compensation term was previously [1, 2, 3, 5, 6, 7] added to the activation energy of viscous flow. The form of that term was developed based on the assumption [47] that the *charge compensation effect* appears when the Al^{3+} replaces Si^{4+} in tetrahedral coordination positions, thus keeping the silicate network structure instead of breaking it. That mechanism related *charge compensation effect* to the presence of the silicate networks. The special *charge compensation term* therefore was previously [1, 2, 3, 4, 5, 6, 7] made proportional to the concentrations of the Si-Si structural units.

That understanding, however, has recently been revised. First, it did not reflect the fact that the maximum of viscosity was observed also in the SiO_2-free systems (e.g. CaO-Al_2O_3 [49, 50]). Second, the silicate slag viscous flow is viewed as the movements of individual Si-Si and other structural units due to the breaks of the individual bonds. The networks in slags are different from the rubber or plastics, they are not permanent and individual Si-Si bonds do break. The viscous flow depends on the strength of the individual Si-Si bonds rather than on the network length. Accepting the suggestion that formation of tetrahedral Al^{3+} influences the strength of the individual bonds in the long networks is to also accept long range (more than several atomic distances) interactions, the latter concept is believed to be incorrect. Instead, the strength of the individual Si-Si bonds is taken to be independent of the formation of the tetrahedral Al^{3+} at a distant atomic position (only the second nearest neighbour interaction is taken to be significant). The presence of a network is not taken to justify high viscosity. The increase of viscosity and the presence of networks both are taken to be the result of the strength of the individual bonds involving tetrahedral Al^{3+}. This assumption means that the increase of viscosity due to the charge

compensation effect is due to the stronger Al-Al and Al-Si bonds for the tetrahedral Al^{3+} and do not depend on the concentrations of the Si-Si bonds, which agrees with experimental evidence [49, 50]. The *charge compensation term* previously used in the viscosity model [1, 2, 3, 4, 5, 6, 7] has therefore been removed and additional parameters describing the effects of Ca^{2+}, Fe^{2+} and Mg^{2+} on the partial activation energies of the Al-Al and Al-Si structural units were allowed to be introduced, and experimental data were described.

In difference with the Ca-, Fe- and Mg-containing systems, for the Na- and K-containing systems following previous suggestion [48] the *charge compensation effect* was introduced in the thermodynamic model through the AlKO and AlNaO associates [23, 51] so that no special viscosity terms were necessary in the viscosity model. Figures 7 and 8 demonstrate agreement with experimental data for the Al-Na-O-Si and Al-K-O-Si systems. Figure 9 provides comparison of the viscosities at SiO_2 = 50 mol % for different oxide melts.

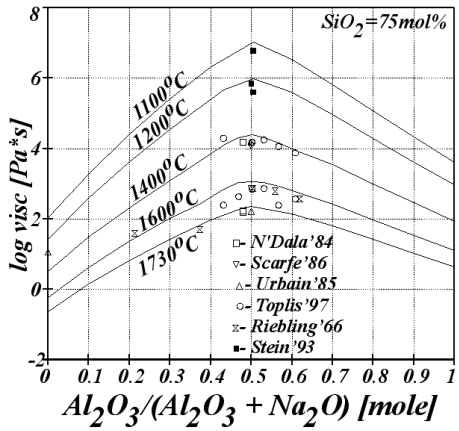

Figure 7: Viscosities in the Al-Na-O-Si system at SiO_2 = 75 mol%

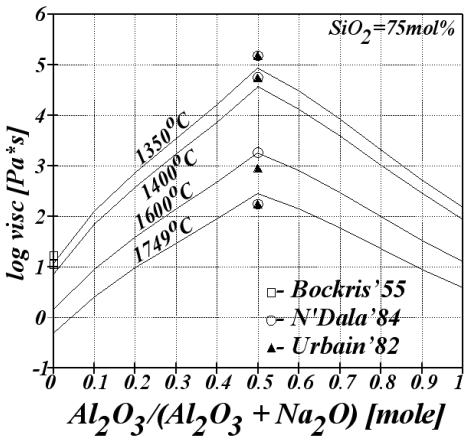

Figure 8: Viscosities in the Al-K-O-Si system at SiO_2 = 75 mol%

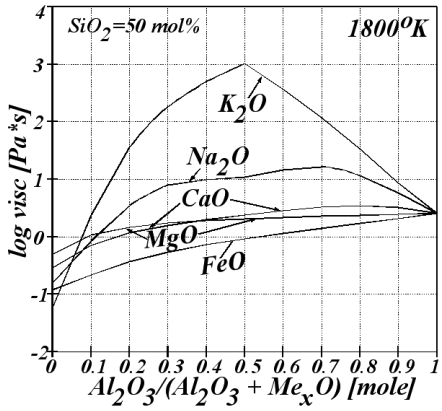

Figure 9: Viscosities in the Al-Me-O-Si systems at SiO_2 = 50 mol% predicted by the present model

Features of the Present Viscosity Model

The present viscosity model requires development of a structurally-based (e.g. quasi-chemical) thermodynamic model using phase equilibria and thermodynamic data. There are a number of helpful features of the present viscosity model. The values of the molar partial activation energies and vaporisation energy coefficients obtained using the experimental data in the binary and ternary systems are extrapolated into higher order systems where no experimental data are available, enabling predictions to be performed and, in some cases, discrepancies between experimental data to be identified. Restrictions are introduced on the model parameters – for example, the sign (positive) and the magnitude of the molar partial and integral activation energies, and molar integral vaporisation energies. The trends in the changes of the model parameters are analysed in the experimentally well-characterised systems; these trends are then used for interpolations and extrapolations in other systems in which experimental data is lacking. The model is flexible enough to reflect major structural changes, but *rigid* for composition ranges with similar structural units distributions. The molar activation and vaporisation energies of the structural units have been *de-convoluted* and can now be analysed and used for other applications.

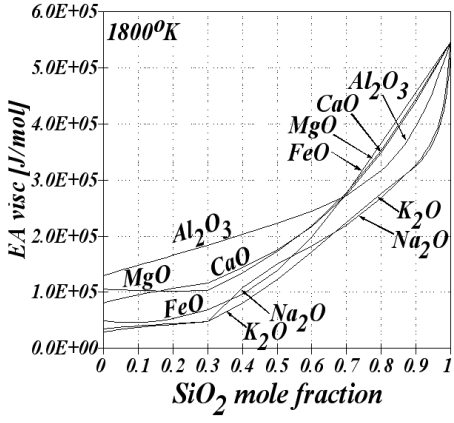

Figure 10: Viscous flow integral molar activation energies in the Me-O-Si systems

A number of trends in the activation energies were identified; examples of these are illustrated in Figure 10 for Al_2O_3-, CaO-, *FeO-* , MgO-, Na_2O- and K_2O-SiO_2 binary systems. i) Si-Si partial activation energy changes significantly with composition (see Figure 11), whereas the Si-Me (Me≠Si) and Me-Me (Me≠Si) (Figure 11) activation energies do not appreciably change. ii) Si parameters are significantly different from Na, K, Fe, Ca, Mg and Al. iii) Model parameters for CaO and MgO are very close to each other and the values of various parameters are generally in the sequence K→Na→Fe→ (Ca or Mg)→ Al (see Table 1). iv) It was found that $E_{a,Me1\text{-}Me2} = ½(E_{a,Me1\text{-}Me1} + E_{a,Me2\text{-}Me2})$, where Me1≠Si, and Me2≠Si, is a reasonable assumption. Similar trends were found for the vaporisation energy parameters. These and some other trends have significantly assisted in the selection of parameters for the systems in which experimental data is lacking and can be further used in other chemical systems. The present thermodynamic model is currently being further revised together with the parameters for the viscosity model. The set of the viscosity model parameters given in Table 1 is preliminary and is further being reviewed.

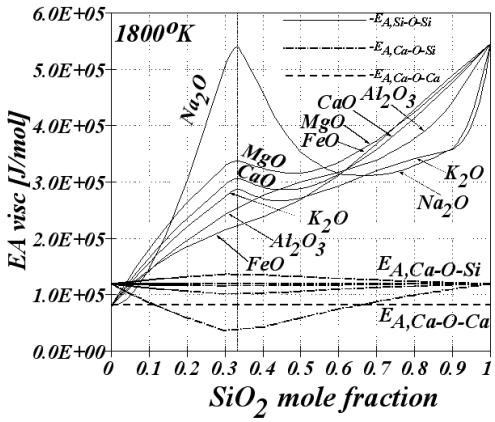

Figure 11: Viscous flow partial molar activation energies in the Me-O-Si systems

INDUSTRIAL APPLICATION OF THE MODEL TO EXAMINE EFFECTS OF ALKALIS ON IRON BLAST FURNACE SLAGS

The development of the model makes it possible to predict slag viscosities in composition ranges where little or no experimental viscosity data are available, particularly in complex industrially important slag systems. In the present paper this point is illustrated with reference to the iron blast furnace slag. It is widely recognized that alkali metals accumulate inside the iron blast furnace through vaporization and condensation (recirculation) and can cause operational problems. A simplified model was developed to predict the behaviour of alkalis in the blast furnace and to examine the effects of changing process variables [51, 52]. The FactSage computer package with macros [21] and a new recently optimized thermodynamic database [22, 23] describing slags in the system Al_2O_3-CaO-FeO-Fe_2O_3-Na_2O-K_2O-MgO-SiO_2 have been used for the blast furnace model [51, 52]. The model describes heat exchange, vaporization of volatile elements in the hearth, associated re-oxidation and condensation reactions in the gas phase during ascent of the gas and resulting re-circulation of volatile elements inside the furnace. Thermodynamic calculations predict the phases formed, and the partitioning of major elements between the solid compounds, liquid oxide, metal and gas phases.

Table 2: Data on Fukuyama No. 5 furnace [53]

Metal production	**9900 tonnes hot metal (THM)/d**
Hearth diam. H_H	14.4 m
Air Blast temp	1550 K
Hearth temp	1800 K
Coke rate	470 kg/THM
Air blast	1040 Nm^3/THM
Slag mass	320 kg/THM
Alkali load in feed (50%Na_2O / 50%K_2O)	10 kg/THM

Assumtions: Fe feed is 100% fluxed sinter.
50% (SiO_2 + Al_2O_3) impurities in sinter 50% in coke at the same Al_2O_3 /SiO_2 ratios
All flux materials CaO, MgO and impurities SiO_2, Al_2O_3, Na_2O, K_2O as oxides
S is not considered in the calculations
Hearth Temperature = slag and metal Temp

Base Slag composition (wt %)
([54], Mannesmann furnace)

SiO_2	**CaO**	**MgO**	**Al_2O_3**
34.63	41.70	6.74	11.57
Al_2O_3/SiO_2	CaO/SiO_2	Approx.T_{liq}	
0.334	1.20	1700 K	

Table 3: Compositions of slags inside blast furnace that were predicted to appear due to accumulation of Na and K

Na and K load Kg/tn metal	**Recir-culation**	**SiO_2 wt%**	**Al_2O_3 wt%**	**CaO wt%**	**K_2O wt%**	**MgO wt%**	**Na_2O wt%**
5	No	40.0	11.3	40.7	0.7	6.6	0.7
	Yes	33.2	9.4	33.7	16.1	5.5	2.2
7.5	No	39.8	11.2	40.3	1.1	6.5	1.1
	Yes	30.5	8.6	30.9	21.9	5.0	3.1
10	No	39.5	11.1	40.0	1.5	6.5	1.5
	Yes	28.1	7.9	28.4	26.9	4.6	4.1

The information on the iron blast furnace used for model development including major feed stream compositions, stream amounts and stream temperatures (see Table 2) was used to tune the model. The model output includes the compositions, amounts and temperatures of the off-gas, slag, and metal streams. Importantly, the extents of the Na and K re-circulation and accumulation inside the furnace were predicted. Table 3 presents compositions of the slags without and with the Na and K accumulation inside the furnace predicted by the model for different Na and K loads of 5, 7.5 and 10 kg per tonne of metal. These predictions indicate that significant changes in slag composition can take place due to the accumulation of Na and K inside the furnace. The viscosities of the series of slag compositions between these two compositions at 1800°K were predicted and are given in Figure 12. It was predicted that the increase of the Na_2O and K_2O in slag initially results in the increase of viscosities followed up by the further decrease of viscosities.

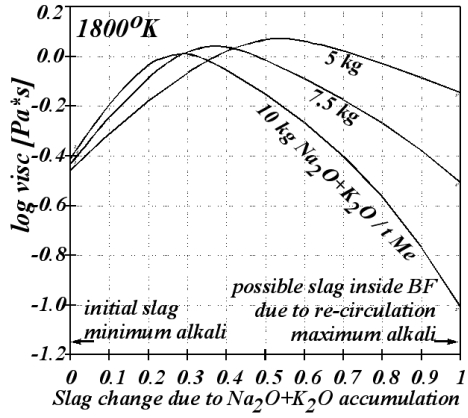

Figure 12: Possible changes to slag viscosities inside the iron blast furnace due to alkali re-circulation (at 1800° K)

SUMMARY

The quasichemical viscosity model has been developed that makes it possible to predict the viscosities of slags in the system Al_2O_3-CaO-*FeO*-MgO-SiO_2-K_2O-Na_2O.

ACKNOWLEDGEMENTS

The author would like to acknowledge essential contribution by Dr A. Kondratiev the key co-developer of this viscosity model over a number of years of work at the Pyrometallurgy Research Centre. The author is grateful to Prof. Peter Hayes for useful critical discussions, suggestions on model development, support and review of the paper. The author thanks Mr Matt Pyle assisting with programming and with the data treatment. The author would like to acknowledge the financial support from the Cooperative Research Centre for Coal in Sustainable Development (CCSD) and the Australian Research Council (ARC) enabling this research to be carried out.

REFERENCES

Kondratiev, A. & Jak, E. (2005). *A Quasi-Chemical Viscosity Model for Fully Liquid Slags in the Al_2O_3-CaO-'FeO'-SiO_2 System*. Met.Trans B, Vol. 36B, pp. 623-638. [1]

Kondratiev, A., Hayes, P. C. & Jak, E. (2005). *Development and Application of a Quasi-Chemical Viscosity Model for Al_2O_3-CaO-"FeO"-MgO-SiO_2 Slags*, 150th ISIJ Int. Meeting, Hiroshima, Japan, Sep 2005, CAMP-ISIJ, Vol. 18(4), pp. 821-825. [2]

Kondratiev, A., Hayes, P. C. & Jak, E. (2006). *Development of a Quasi-Chemical Viscosity Model for Fully Liquid Slags in the Al_2O_3-CaO-'FeO'-MgO-SiO_2 System*. Part 1. Description of the Model and its Application to the MgO, MgO-SiO_2, Al_2O_3-MgO and CaO-MgO Sub-systems, ISIJ International, Vol. 46, No. 3, pp. 359-367. [3]

Kondratiev, A., Hayes, P. C. & Jak, E. (2006). *Development of a Quasi-Chemical Viscosity Model for Fully Liquid Slags in the Al_2O_3-CaO-'FeO'-MgO-SiO_2 System*. Part 2. A Review of the Experimental Data and the Model Predictions for the Al_2O_3-CaO-MgO, CaO-MgO-SiO_2 and Al_2O_3-MgO-SiO_2 Systems, ISIJ International, Vol. 46, No. 3, pp. 368-374. [4]

Kondratiev, A., Hayes, P. C. & Jak, E. (2006) *Development of a Quasi-Chemical Viscosity Model for Fully Liquid Slags in the Al_2O_3-CaO-'FeO'-MgO-SiO_2 System*. Part 3. Summary of the Model Predictions for the Al_2O_3-CaO-MgO-SiO_2 System and its Sub-systems, ISIJ Int., Vol. 46, No. 3, pp. 375-384. [5]

Kondratiev, A., Hayes, P. C. & Jak, E. (2008). *Development of a Quasi-Chemical Viscosity Model for Fully Liquid Slags in the Al_2O_3-CaO-'FeO'-MgO-SiO_2 System*. Part 4. The Experimental Data for the 'FeO'-MgO-SiO_2, CaO-'FeO'-MgO-SiO_2 and Al_2O_3-CaO-'FeO'-MgO-SiO_2 Systems at Iron Saturation, ISIJ International, 48(1), 7-16. [6]

Kondratiev, A., Hayes, P. C. & Jak, E. (2008). *Research Report 88 Slag Viscosity Prediction for Applications in Coal Gasification (The Quasi-Chemical Viscosity Model for the System Al_2O_3-CaO-'FeO'-K_2O-MgO-Na_2O-SiO_2)*. The University of Queensland, Centre for Coal in Sustainable Development, Brisbane, Australia, www.ccsd.biz. [7]

Grundy, A. N., Liu, H., Jung, In-Ho., Decterov, S. A. & Pelton, A. D. *A Model to Calculate the Viscosity of Silicate Melts*. Part I: Viscosity of Binary SiO_2-MeOx Systems (Me = Na, K, Ca, Mg, Al), Int.J.of Materials Research (formerly:Zeitschrift fuer Metallkunde),in Press. [8]

Grundy, A. N., Liu, H., Jung, In-Ho., Pelton, A. D. & Decterov, S. A. *A Model to Calculate the Viscosity of Silicate Melts*. Part II: The $NaO_{0.5}$-MgO-CaO-$AlO_{1.5}$-SiO_2 System, Int. J. of Materials Research (formerly:Zeitschrift fuer Metallkunde),in Press. [9]

Zhang, L. & Jahanshahi, S. (1998). Met.Mater.Trans. B, Vol. 29B, pp. 177-186 ibid. pp. 187-195. [10]

Tanaka, T., Nakamoto, M., Lee, J. & Usui, T. (2003). Sci. Tech. Innovative Ironmaking Aiming Energy Half Consump., 161. [11]

Frenkel, J. (1946). *Kinetic Theory of Liquids*. Oxford University Press, UK. [12]

Glasstone, S., Laidler, K. J. & Eyring, H. (1941). *Theory of the Rate Processes*. McGraw-Hill, NY. [13]

Kingery, W. D., Bowen, H. K., & Uhlmann, D. R. (1976). *Introduction to Ceramics*. John Wiley & Sons, Toronto. [14]

Waseda, Y. & Toguri, J. M. (1998). *The Structure and Properties of Oxide Melts*. World Scientific, Singapore. [15]

Fincham, J. B. & Richardson, F. D. (1954). Proc. Royal Soc. (London), Vol. 223, pp. 40-62. [16]

Shannon, R. D. (1976). Acta Crystallographica, Vol. A32, pp. 751-767. [17]

Blander, M. & Pelton, A. D. (1984). 2nd Int. Symp. Metal. Slags Fluxes, TMS-AIME, Warrendale, PA, pp. 295-304. [18]

Pelton, A. D., Decterov, S. A., Eriksson, G., Robelin, C. & Dessureault, Y. (2000). *The Modified Quasichemical Model. I—Binary Solutions*. Metall. Mater. Trans. B, Vol. 31B pp. 651–659. [19]

Pelton, A. D. & Chartrand, P. (2001). *The Modified Quasichemical Model. II-Multicomponent Solutions*. Metall. Mater. Trans. A, Vol. 32A. pp. 1355-1360. [20]

FactSage (2008). Ecole Polytechnique, Montréal, http://www.factsage.com/. [21]

Decterov, S. A., Jung, I. H., Jak, E., Kang, Y. B., Hayes, P. C. & Pelton, A. D. (2004). 7th Int Conf Molten Slags Fluxes Salts, Cape Town, South Africa, publ. SAIMM, Johannesburg, SA, pp. 839-850. [22]

Jak, E. & Hayes, P. C. (2004). Final report, *Prediction of Liquidus Temperatures and High Temperature Phase Equilibria for the System SiO_2-Al_2O_3-FeO-Fe_2O_3-CaO with Addition of Na_2O-K_2O-MgO*. The University of Queensland, Centre for Coal in Sustainable Development (CCSD), Brisbane, Australia, www.ccsd.biz. [23]

ChemApp (2008). GTT Technologies, Germany, http://www.gtt-technologies.de/. [24]

Eipeltauer, E. & Jangg, G. (1955). *Über die Beziehung zwischen Viskosität und Zusammensetzung Binärer Natriumsilikatgläser I*. Kolloid Zeitschrift und Zeitschrift für Polymere, 142, pp. 77-84. [25]

Heidtkamp, G. & Endell, K. (1936). *The Dependence of Density and Viscosity on Temperature in the System Soda-Silica*. Glastechnische Berichte., 14, pp. 89-103. [26]

Knoche, R., Dingwell, D. B., Seifert, F. A. & Webb, S. L. (1994). *Non-linear Properties of Supercooled Liquids in the System Na_2O-SiO_2*. Chemical Geology., 116, pp. 1-16. [27]

Lillie, H. R. (1939). High-temperature Viscosities of Soda-Silica Glasses. *Journal of the American Ceramic Society*, 22, pp. 367-374. [28]

Preston, E. (1938). The Viscosity of the Soda-Silica Glasses at High Temperatures and its Bearing on their Constitution. *Journal of the Society of Glass Technology*. 22, pp. 45-82. [29]

Sasek, L., Meissnerova, H. & Prochazka, J. (1975). *Struktura a Vlastnosti Kremicitych Tavenin*. 7. Porovnani Vlivu Velikosti Iontu Me+ a Me++ na Viskozitu Kremicitych Sklovin., Sbornik Vysoke Skoly Chemicko-Technologicke v Praze. Chemie a technologie silikatu., Schientific Papers of the Prague Institute of Chemical Technology. Chemistry and Technology of Silicates, L6, pp. 95-129. [30]

Shvaiko-Shvaikovskaya, T. P., Mazurin, O. V. & Bashun, Z. S. (1971). *Viscosity of Sodium Oxide-Silicon Dioxide System Glasses in Molten State*. Izvestiya Akademii Nauk SSSR. Neorganicheskiye Materialy., 7, 1, pp. 143-147. [31]

Bockris, J. O'M., MacKenzie, J. D. & Kitchener, J. A. (1955). *Viscous Flow in Silica and Binary Liquid Silicates*. Transactions of the Faraday Society, 51, pp. 1734-1748. [32]

Shartsis, L., Spinner, S. & Capps, W. (1952). Density, Expansivity and Viscosity of Molten Alkali Silicates, *Journal of the American Ceramic Society*. 35, pp. 155-160. [33]

Urbain, G. (1985). *Viscosité de Liquides Silice-Alumine-Oxydes Na et K. Mesures et Estimations*. Revue Internationale des Hautes Temperatures et des Refractories, 22, pp. 39-45. [34]

Sasek, L. (1977). *The Viscosity of Silicate Glass Melts*. Silikaty., 21, pp. 291-305. [35]

Mizoguchi, K., Okamoto, K. & Suginohara, Y. (1982). *Oxygen Coordination of Al^{3+} Ion in Several Silicate Melts Studied by Viscosity Measurements*. J. of the Japan Inst. Metals, 46, pp. 1055-1060. [36]

Urbain, G. (1985). J. Mater. Educ., Vol. 7, pp. 1007-1078. [37]

Mills, K. C. (1995). *Slag Atlas*, 2nd edition, Verlag Stahleisen GmbH, Düsseldorf. [38]

Urbain, G., Bottinga, Y. & Richet, P. (1982). Geochim. Cosmochim. Acta, Vol. 46, pp. 1061-1072. [39]

Kozakevitch, P. (1960). Rev. Metall., Vol. 57, pp. 149-160. [40]

Urbain, G., Bottinga, Y. & Richet, P. (1982). *Viscosity of Liquid Silica, Silicates and Alumino-Silica, Geochimica et Cosmochimica Acta*. 46, pp. 1061-1072. [41]

N'Dala, I., Cambier, F., Anseau, M. R. & Urbain G. (1984) *Viscosity of Liquid Feldspars*. Part I: Viscosity Measurements, Trans.and J.of the British Ceram.Soc., British Ceram. Abstr., 83, pp. 105-107. [42]

Scarfe, C. M. & Cronin, D. J. (1986). *Viscosity-temperature Relationships of Melts at 1 Atm in the System Diopside-Albite*. The American Mineralogist., 71, pp. 767-771. [43]

Toplis, M. J., Dingwell, D. B. & Lenci, T. (1997). *Peraluminous Viscosity Maxima in Na_2O-Al_2O_3-SiO_2 Liquids: The Role of Triclusters in Tectosilicate Melts*. Geochimica et Cosmochimica Acta., 61, pp. 2605-2612. [44]

Riebling, E. F. (1966). Structure of Sodium Aluminosilicate Melts Containing at Least 50 mole % SiO_2 at 1500C. *Journal of Chemical Physics*, 44, pp. 2857-2865. [45]

Stein, D. J. & Spera, F. J. (1993) Experimental Rheometry of Melts and Supercooled Liquids in the System $NaAlSiO_4$-SiO_2: Implications for Structure and Dynamics, The Am. Miner., 78, pp. 710-728. [46]

Mysen, B. O. (1988). Dev. Geochem., Vol. 4, pp. 1-354. [47]

Chartrand, P. & Pelton, A. D. (1999) Calphad, Vol. 23, pp. 219-230. [48]

Hofmaier, G. (1968). *Berg und Huttenm*. Monatsh. Montan. Hochschule Loeben,v.113,pp.270-281. [49]

Urbain, G. (1983). Rev. Int. Haut. Temp. Refract., Vol. 20, pp. 135-139. [50]

Jak, E., Hayes, P. C., Pelton, A. D. & Decterov, S. A. (2009). *Thermodynamic Modelling of the Al_2O_3-CaO-FeO-Fe_2O_3-PbO-SiO_2-ZnO System with Addition of K and Na with Metallurgical Applications*. Molten Chile. [51]

Jak & Hayes. (2008). *The Use of Thermodynamic Modeling to Examine Alkali Recirculation in the Iron Blast Furnace*. Japan-Australia-China Workshop on Iron and Steelmaking, Kyoto, Japan. [52]

Peacey, J. G. & Davenport, W. G. (1979). *The Iron Blast Furnace–Theory and Practice*. Pergamon. [53]

Biswas, A. K. (1981). *Principles of Blast Furnace Ironmaking – Theory and Practice*. SBA Publications, Calcutta, India. [54]

Frenkel, J. (1926). Z. Phys., Vol. 35, pp. 652-669. [55]

Frenkel, J. (1937). Trans. Faraday Soc., Vol. 33, pp. 58-65. [56]

Eyring, H. (1936). J. Chem. Phys., Vol. 4, pp. 283-291. [57]

Ewell, R. & Eyring, H. (1937). J. Chem. Phys., Vol. 5, pp. 726-736. [58]